AIAA JOURNAL
Vol. 41, No. 7, July 2003

Noise Characteristics of Aircraft High Lift Systems

Y. P. Guo*
The Boeing Company, Huntington Beach, California 92647
and
M. C. Joshi†
The Boeing Company, Seattle, Washington 98124

The characteristics of far-field noise from aircraft high lift systems are discussed. Analyses are made of the data from an airframe noise test conducted in the 40 by 80 ft wind tunnel at NASA Ames Research Center, using a 4.7% DC-10 aircraft model. Discussions are given on both far-field free microphone data and measurements from a phased microphone array. Major trends are revealed and discussed from the free microphone data, which include far-field frequency characteristics, dependence of the acoustic radiation on flow Mach numbers, effects of flap and/or slat deployment, and far-field directivity. Data from the phased microphone array are used to identify locations of major noise sources. Four subregions on the wing are identified as important source locations, namely, the leading-edge slat region, the inboard and outboard side edges of the outboard flap, and the inboard flap region close to the hub of the wing. The source strength distributions in these subregions are integrated to reveal dependencies of various noise sources on flow conditions and high lift system configurations. The effects of flap side edge fences on far-field noise are also discussed, which shows a reduction of a few decibels in flap-related noise.

I. Introduction

AIRFRAME noise has long been known to contribute significantly to the total aircraft noise, especially for commercial wide-body aircraft at landing approach.[1–4] A major source of airframe noise is believed to be associated with the flow in the vicinity of the aircraft high lift system. At landing approach when the high lift systems, namely, the flaps and slats, are deployed, the flow becomes very complex, involving phenomena such as flow separation and shear-layer instability both in the slat region and near the side edges of the flaps. These complex flow features inevitably cause flow fluctuations that can escape to the far field as sound. To help understand the noise source mechanisms associated with these flow features and their far-field characteristics, an acoustic test was conducted in the 40 by 80 ft wind tunnel at NASA Ames Research Center, using a 4.7% DC-10 model aircraft. In this paper we discuss the noise characteristics of aircraft high lift systems by presenting the analysis of the data from that test. The test facility and measurement implementation will be described in Sec. II. The far-field measurements include sound-pressure spectra and directivities by free field microphones and noise source amplitudes by a phased microphone array. In addition to far-field measurements, fluctuations of surface pressures are also measured by unsteady pressure sensors, which are implemented on the components of the high lift systems. The analysis of the unsteady surface pressures, including their correlation with far-field noise, has been reported elsewhere,[5] but the far-field noise characteristics will be the main focus here.

Aircraft high lift systems consist of many sharp edges and corners, the trailing edges of its components, the cusps of the slats and the side edges of the flaps, for example. Because of this, airframe noise has in the past been characterized by a Mach-number dependence of the fifth power law,[2,4,6] based on the theory of trailing-edge scattering.[7,8] This fifth power law might well explain the noise from clean wing configurations, where the flaps and slats are retracted, and hence, the trailing edges of the wing are the dominant source mechanism. Our data for configurations with fully deployed flats and slats, however, do not comply with this simple scaling law, essentially because the trailing-edge scattering becomes less important in comparison with sources introduced by the flaps and slats. We will show that, while low-frequency noise basically scales on flow Mach number to the fifth power, high-frequency components are governed by the sixth-power law. This dependence of Mach-number scaling law on frequency can appear to be puzzling at first glance but can be readily explained by the existence of multiple sources associated with aircraft high lift systems and by the broadband nature of the noise sources.

It is known that high lift system noise in the low-to-midfrequency domain (below 2 kHz full scale, say) is dominated by sources in the slat region, probably associated with flow separation in the slat cove.[9] In this case the flow can be approximated as two dimensional, leading to noise source distributions along the spanwise direction of the slats. This will be confirmed by our source strength data from the phased microphone array. For these two-dimensional sources the far-field radiation scales on the fifth power law.[10–12] This fifth power scaling law results entirely from the two-dimensional nature of the sources and holds without the mechanism of shape edge scattering. In the high-frequency domain airframe noise dominantly comes from the flow in the vicinity of flap side edges, associated with flow separation in the flap crossflow.[4,13–15] Because these sources are very broadband, covering the range from 1 to 100 kHz in our model test, the acoustic wavelengths vary quite significantly within this frequency range, covering two decades. Thus, in terms of the acoustic wavelength, the sources can be regarded as being both "very close to" and "very far away from" any flap side edges, respectively, at low and high frequencies, even though they are located at fixed physical locations in relation to the edges. This is because the sources are close if they are within one wavelength distance from the edge but far away if they are more than one wavelength away. For the former, the closeness to the edge, in terms of wavelength, makes the radiation to be dominated by sharp edge diffraction, leading to the fifth power law.[7] For the latter, the distance of many wavelengths makes the sources behave effectively unaware of the edges, in which case the radiation follows the sixth power law of dipole radiation.[16,17] This also explains the Mach-number dependence observed in aircraft flyover tests; noise data for flap-related high-frequency components have been shown to scale on a power law of approximately 5.8 for a series of Boeing aircraft.[18]

As typically observed for airframe noise,[2,6,18,19] our data will show a very broad far-field directivity pattern. The maximum

Received 28 June 2002; revision received 17 January 2003; accepted for publication 4 February 2003.

*Senior Principal Engineer, Mail Code H013-B308, Boeing Phantom Works. Member AIAA.
†Manager, Mail Code 67-MK, Boeing Commercial Airplane Company. Member AIAA.

radiation occurs in the fly-over direction right below the aircraft, but the falloff away from this direction is very gradual. Even at positions 60 deg away from this maximum radiation direction, the noise levels are still within 5 dB of the maximum. This broad directivity pattern results again from the existence of multiple sources associated with the high lift systems. As analyzed in Refs. 5 and 9, sources related to slats and flaps have maximum radiation in different directions. For slat sources the maximum radiation is in the aft quadrant, whereas for the flap sources the maximum occurs in the forward quadrant. The aggregated effects of all of these sources then lead to the broad directivity.

We will show that noise levels are also dependent on the high lift system configurations, as can be intuitively expected. In general, deployment of any components (slat or flap) increases the far-field noise level and the larger the deployment angle, the higher the noise. The changes in noise levels with the high lift system components are, however, frequency dependent. It is found that the deployment of slats mainly increases noise in the midfrequency domain. When the slats are deployed at 20 deg, the noise level is increased, from the case with slats retracted, up to about 4 dB within the frequency band from 1 to 30 kHz. This covers approximately the frequency band between 100 and 2.5 kHz in full scale. For flaps, increasing flap angle affects almost the entire mid- and high-frequency domain with the most significant effects at high frequencies. When the flap angle increases from 0 to 50 deg, the increase in noise level can be as high as 10 dB at high frequencies when the flaps are the only sources, namely, when the slats are retracted. When both flaps and slats are deployed, the increase in noise levels caused by flap angle increase is somewhat less significant because the slat contributions make the noise levels already high at small flap angles. These trends are completely consistent with previously published data, both for the same DC-10 aircraft model at full scale[19] and for other types of aircraft.[18]

In recent years the technology of phased microphone arrays has found many applications in aircraft noise research.[20,21] The technology is known to be especially helpful in locating noise sources. We will show that major sources can be identified at the side edges of the flap, appearing as quite concentrated sources, and in the slat region, as distributed sources. The strengths of the sources vary with frequency because different sources dominate in different frequency domains. Similar to the noise they generate, the sources also depend on the high lift system configurations. This will be discussed in detail by analyzing the effects of changes in the flap/slat configurations on the integrated source strengths in different regions in the high lift system. Compared with the analysis on the total far-field noise, this has the advantage of explicitly bringing out the effects of different sources. For example, the integrated source strength for the slat region will be shown to be almost independent of the flap deployment angle, although the total far-field noise shows a strong dependence on this angle at high frequencies. This implies that the high-frequency components of the total noise are dominantly radiated by sources related to the flaps. Similarly, it will be shown that flap sources are much less affected by changes in the slat deployment angle than those related to the slats. We choose to work with the integrated source strength because it is a more accurate measure of the effects on the far-field radiation than the individual source levels. This will be clearly demonstrated by the comparison between slat sources and flap sources. The beam-forming results of the phased microphone array show that the levels of the sources in the slat region are much lower than those associated with the flap side edges. This does not, however, necessarily mean that slat sources radiate less because the slat sources are distributed over a large spatial domain, whereas the flap sources are highly concentrated. Indeed, we will show that when integrated over their respectively regions the two kinds of sources have comparable strengths, indicating their comparable importance in noise radiation.

With the identification of the flap side edges as one of the major noise sources, noise reduction concepts have in recent years been studied, one of them being flap side edge fences.[21,22] Devices like this seek to modify the flow features in the flap side edge region favorably and, thus, achieve noise reduction. Although the exact mechanisms by which flap-related noise is reduced by side edge fences are not fully understood, the effectiveness of the fences in reducing flap-related noise has been demonstrated. This will be confirmed by our test data, which show a quite noticeable reduction in noise levels in the entire mid- to high-frequency domain, corresponding to up to a 4-dB reduction in the effective perceived noise level (EPNL). It is, however, appropriate to point out that the reduction is for flap-related noise only; in the case of total aircraft noise consisting of many other components, the reduction in EPNL decibels can be expected to be much less. This is especially true for cases where there are other major sources present, such as those related to the slats, which are almost unaffected by flap side edge fences. Indeed, our data will show that, at low-to-moderate flap settings, as is often the case for modern aircraft, a significant amount of the total airframe noise comes from the slat-related sources. In this case the total airframe noise would not be very sensitive to flap side edge treatment such as fences.

II. Test Facility, Measurement Implementation, and Data Analysis

The aircraft model used in our test is a 4.7% small-scale model of the McDonnell Douglas DC-10-30 transport airplane. Its high lift system consists of two partial-span, single-element slats and two partial-span, single-element flaps, which are, respectively, called the inboard and the outboard slat/flap. The engines on the small-scale aircraft are modeled as flow-through device without power. Both the slats and the flaps on the small model are adjustable. The model has a wingspan of approximately 8 ft (2.4384 m), and it is a true scale-down of the DC-10 configuration; the small-scale model has all of the components, including all the stabilizers and landing gears. A schematic drawing of the aircraft configuration is shown in Fig. 1. The tests, together with some data analysis, have also been previously described,[23] and a similar test with the same aircraft type has also been reported.[24]

The test facility is the 40 by 80 ft wind tunnel at NASA Ames Research Center, which is a closed flow facility with partial acoustic treatment. The model is mounted with a sting connected with a knife-blade-type support. The height of the model in the facility was determined by reproducing the Federal Aviation Administration fly-over altitude of 394 ft (120 m) at model scale. A sting mount was chosen to provide as great a distance as possible between the support system and the model to reduce the potential contamination of the radiated noise measurements by noise generated on the

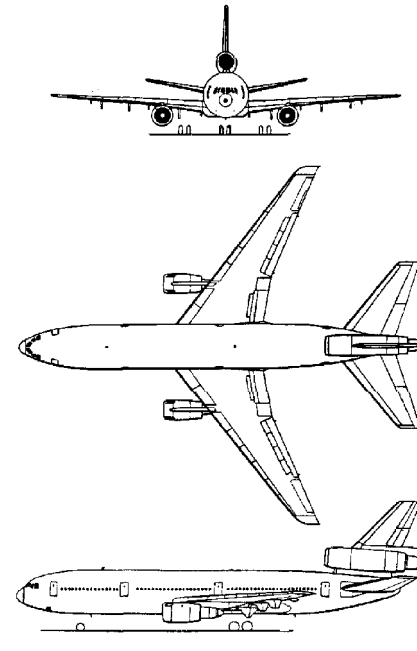

Fig. 1 Schematics of the McDonnell Douglas DC-10 transport aircraft.

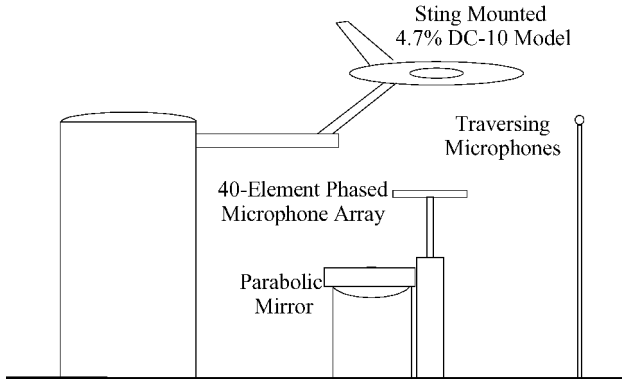

Fig. 2 Test setup for the 4.7% DC-10 model in the 40 by 80 ft wind tunnel in NASA Ames Research Center.

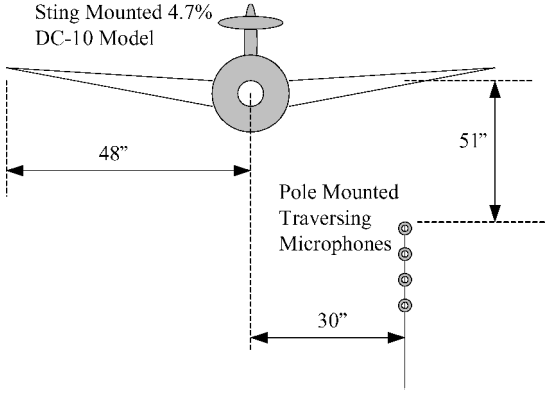

Fig. 3 Locations of far-field free microphones traversing parallel to the mean flow.

support. The test section with the 4.7% DC-10 model is illustrated in Fig. 2, together with the instrumentation of the noise measurements. These include two pairs of pole-mounted traversing microphones, a phased microphone array of 40 elements, and an array of six parabolic acoustic mirrors mounted in a fairing directly below the model. The results and analysis given in this paper are based on the free-field microphone data and the phased microphone array measurements. The locations of the pole-mounted free-field microphones are shown in Fig. 3. It is positioned right below the outboard edge of the outboard flap, which was anticipated to be a major noise source location. The pole-mounted microphones can be traversed in the direction parallel to the wind-tunnel flow, providing directivity measurements. The traversing microphones are B&K 0.25-in. type fitted with wind screen nose cones developed by NASA Ames Research Center, Moffett Field, California.[22] Each pair of microphones is 4 in. (0.1 m) apart with a 4-ft (1.2-m) separation distance between the two pairs. The microphones are calibrated with a piston-phone before each test.

The tests are done for various aircraft configurations and flow conditions with the angle of attack of the wing fixed at 5 deg. There are altogether 33 runs in which far-field noise was measured. The parameters relevant to the discussion in this paper are the mean-flow Mach number M, the flap angle δ_F, and the slat angle δ_S. The values of these parameters used in the test are summarized here:

$$M = 0.2, 0.25, 0.275$$
$$\delta_F = 0, 25, 35, 50 \text{ deg}$$
$$\delta_S = 0, 20 \text{ deg} \tag{1}$$

where the value of 0 deg means the component is retracted. Landing gears are also modeled on the small-scale aircraft and are tested both on and off. The size of the model gears, however, does not allow a true scale-down of the real landing gears. The small model landing gear only has the major components (struts and wheels), which cannot be expected to capture the most important mid- to high-frequency noise generated by the smaller components of the gear assembly. Our data basically show no significant difference between gear-on and gear-off configurations for the small model, in contrast to the known fact that landing gear is a major source of airframe noise for real aircraft. This indicates that the variations caused by the deployment of the small gears might not be reliable, and so no results will be presented here. Also tested are flap side edge fences. They are basically extension plates vertically attached to the side edges of the flap. They are contoured exactly the same on the top side as the upper surface of the flap so that their top sides are flash mounted with the upper surfaces of the flaps. The lower sides of the fences extend beyond the lower surface contours of the flaps so that the crossflow is blocked by the fences. The fences are characterized by their height h, which is defined by the part extending into the flow. Three values of h are tested, namely,

$$h = 0.5t_F, 1.0t_F, 2.0t_F \tag{2}$$

where t_F is the maximum flap thickness at the side edges. Some other changes are also made in the tests, such as sealing the hinges and fairing the flaps, but no significant effects are found in the data because of these configuration variations. Boundary-layer tripping is also tested on various components to ensure fully developed turbulent boundary-layer flow. Again, comparisons with nontripped cases do not reveal any noticeable effects.

The far-field noise signals are measured and processed with up to 100 kHz of usable data. The data are preprocessed by NASA Ames Research Center, including removing electrical noise tones and applying corrections for microphone gain, prewhitening, and microphone frequency response, as well as free-field correction, nose cone interaction correction, and test-day atmospheric condition correction. The data reduction from time-domain measurements to spectra is done by standard fast Fourier transform with ensemble averaging, which is assumed to be equivalent to time averaging because the noise generation is statistically stationary. The high-speed data acquisition system allows a large number of ensemble averages, and all of the final results are statistically convergent. The details of the data reduction have been previously reported.[23–25] After the initial data reduction the data are then stored as sound-pressure level (SPL) both in $\frac{1}{3}$ octave-band and in narrowband (64-Hz) format for later analysis. The phased microphone array consists of 40 B&K microphones of $\frac{1}{4}$-in. (0.635-cm) diameter. Details of the array design and data-processing technique can be found in Ref. 20, and so they will not be repeated here. Because of limitations in the data acquisition equipment, the frequency range is limited to 20 kHz, which scales to approximately 2 kHz on the full-scale aircraft. This limits the overall usefulness of this technique for discerning all potential noise sources on the real aircraft but still allows an insight into a reasonable portion of the important frequency range.

Although the wind tunnel is only partially treated with sound-absorbing materials, we find quite satisfactory signal-to-noise ratio for the far-field measurements. Because our objective is to study noise from the high lift systems, it is important to make sure that all other potential noise sources contribute only small amounts of noise, in comparison with those from the high lift systems. These include the flow over the fuselage, as well as the tunnel background noise. For this purpose noise levels are measured with only the fuselage in the flow. This is taken as the total background noise and is found to be much lower than the levels with the high lift systems deployed, indicating a satisfactory signal-to-noise ratio. An example of this comparison is shown in Fig. 4 for $M = 0.275$. Plotted in Fig. 4 is the noise spectrum in decibels, defined by

$$10 \log \frac{\Pi(f)\Delta f}{(20\,\mu\text{Pa})^2} \tag{3}$$

where Π is the far-field pressure spectra, a function of frequency f, and Δf is the frequency band equal to 64 Hz. It is clear from Fig. 4 that when the flaps and slats are deployed the noise level is more than 10 dB higher than the background for most frequencies. The difference becomes smaller as frequency decreases, to a minimum of about 5 dB. However, this is not a real concern because for aircraft noise certification the low-frequency components are lightly

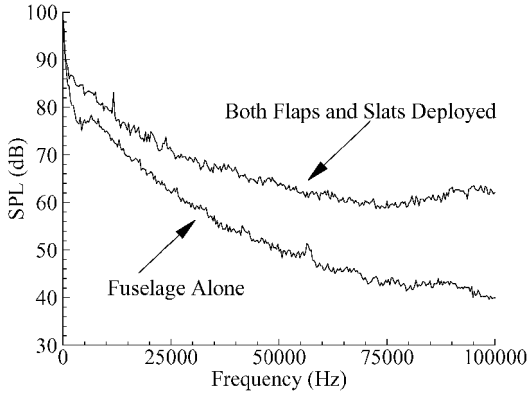

Fig. 4 Comparison of noise spectra between the case with fuselage alone and that with both flaps and slats deployed but landing gears retracted, both for $M = 0.275$.

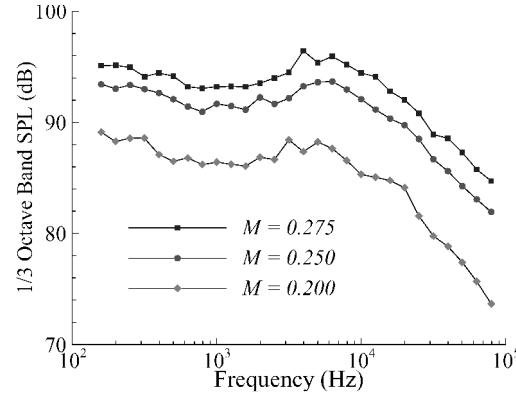

Fig. 5 Far-field noise spectra below the wing (84 deg from upstream direction) at different mean flow Mach numbers with flaps and slats, respectively, deployed at 50 and 20 deg and landing gears retracted.

weighted and, hence, are not important contributors to the total noise levels.

III. Mach-Number Dependence of Far-Field Noise

Our data show very consistent variations with flow Mach number for various aircraft configurations. Some examples are shown in Fig. 5, which plots the $\frac{1}{3}$-octave SPL as a function of frequency at three flow Mach numbers, namely, $M = 0.275$, 0.25, and 0.2. In this case the flaps and slats are, respectively, deployed at 50 and 20 deg, and landing gears are retracted. Evidently, far-field noise levels show strong dependence on the flow Mach numbers, and they increase as the flow Mach number increases. When trying to collapse the data by scaling out the Mach-number dependence, we find that the noise levels do not scale on a single Mach-number law. Instead, low-frequency components approximately scale on the fifth-power law, but the high-frequency components follow the sixth power law. To illustrate this, the noise spectra are integrated over different frequency bands to derive the overall sound pressure levels in these bands. Figure 6 shows the results corresponding to the case shown in Fig. 5. The spectra are divided into two frequency bands, a lower band between 100 Hz and 10 kHz and a higher frequency band between 10 and 100 kHz. The overall sound pressure levels are normalized, respectively, by the fifth and the sixth power law for the two frequency bands. This yields the nondimensional quantity

$$10\log\int_{f_1}^{f_2}\Pi(f)\,\mathrm{d}f - 20\log(20\,\mu\mathrm{Pa}) - 10n\log M \qquad (4)$$

where f_1 and f_2 are, respectively, the lower and upper limit of the frequency band in which the overall SPLs are integrated and n is the power index of the Mach-number scaling law used to collapse the data in the band. Thus, we have

$$f_1 = 100\,\mathrm{Hz}, \qquad f_2 = 10\,\mathrm{kHz}, \qquad n = 5 \qquad (5)$$

for the lower frequency band and

$$f_1 = 10\,\mathrm{kHz}, \qquad f_2 = 100\,\mathrm{kHz}, \qquad n = 6 \qquad (6)$$

for the higher frequency band. The results according to Eq. (4) are plotted in Fig. 6 as a function of the far-field directivity angle, measured from the upstream direction. Clearly, the data collapse quite satisfactorily for each frequency band.

The reason for the different Mach-number scaling laws in different frequency bands is the existence of multiple sources in the high lift systems and the broadband nature of these sources. The latter is clearly seen in the results plotted in Figs. 4–6; the noise spectra cover a wide frequency range from about 100 Hz up to about 100 kHz. Within this frequency range the acoustic wavelengths correspondingly cover three decades. This makes the sources behave quite differently at different frequencies because the source characteristics are governed by the closeness of the sources to features of

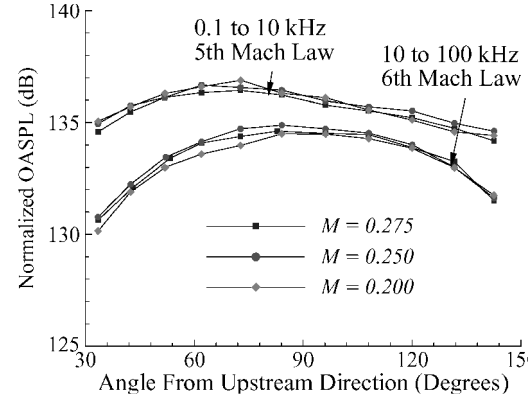

Fig. 6 Normalized overall sound-pressure levels, respectively, for the lower (100 Hz to 10 kHz) and higher (10 to 100 kHz) frequency band at different flow Mach numbers, for the case of flaps and slats, respectively, deployed at 50 and 20 deg and landing gears retracted.

the high lift systems, such as shape edges and corners. This closeness is measured by the typical wavelength of the source fluctuations. For example, the behavior of an unsteady source in the flow at a fixed location in relation to a sharp edge of the high lift system is determined by whether the distance between the source and the edge is smaller or larger than one wavelength. For a broadband source covering a wide range of frequencies, such as those for airframe noise, the source can be both very close to and far away from the edge, measured in terms of the typical wavelength. At low frequencies the wavelength is long so that the source can be within one wavelength from the edge, in which case the radiation is dominated by sharp edge diffraction that is typically governed by the fifth Mach-number power law.[7] In the high-frequency domain where the wavelength is small, the same source can be many wavelengths away from the edge so that the source is essentially unaware of the edge. In this case the sixth power law for Mach number dependence holds because in this case the radiation is typically controlled by the unsteady forces on the high lift system, corresponding to acoustic dipoles.[16,17] Thus, a broadband source can be expected to have radiation scaled on different Mach-number laws at different frequencies. This is clearly the case for the results shown in Fig. 6. The sixth power law for high frequencies has in fact been observed in fly-over data for various Boeing aircraft,[18] where a power law of 5.8 is reported for high-frequency noise dominated by flap sources.

The interpretation of the Mach-number scaling for airframe noise can be further complicated by the sources associated with the leading-edge slats. Although our data and previous studies show the dominance of the slat sources and the scaling of their radiation on the fifth power law in the low- to mid-frequency domain, the mechanisms that lead to this scaling law are much less clear. In the

past airframe noise has been scaled on the fifth power law,[2,6] based on the theory of sharp trailing scattering.[7,8] As pointed in Ref. 4, this might be true only for noise from clean wing configurations where the high lift systems are not deployed and the trailing edges of the wing provide the dominant noise mechanism. For the cases where the flaps and slats are deployed, trailing-edge noise is commonly known to be less important, in comparison with those from sources such as flap side edges and slats. This will also be confirmed by our data from the phased microphone array in a later section. Thus, it is not clear whether the sharp edge scattering can satisfactorily explain the fifth power law for the Mach-number dependence of the far-field noise. An alternative explanation might be provided by the distributed nature of the slat-related sources. As will be shown in a later section, our data from the phased microphone array show that the sources occupy almost the entire slat region. For frequencies of interest to aircraft noise, the typical wavelengths are much smaller than the spanwise dimensions of the slats. If the flow features in the slat region have coherence lengths larger than the typical acoustic wavelength, the slat-related noise sources can be approximated as two dimensional. In this case the two-dimensional sources cause radiation that scales on the fifth power law of flow Mach numbers.[10–12] This fifth power scaling law holds without any sharp edge scattering and results entirely from the two-dimensional nature of the sources. A theory for such sources is proposed,[9] in which slat-related noise is attributed to the unsteady flow separation in the slat cove region. In that study Kutta conditions are imposed at all sharp edges and cusps on the slats so that the scattering mechanism underlining the Ffowcs Williams and Hall theory is absent. Because of the lack of flow measurements in the slat region in our tests, we cannot conclusively show the relation between the spanwise correlation length of the flow features and the acoustic wavelength, and hence, cannot conclusively demonstrate the two dimensionality of the slat-related sources. Further research is apparently needed.

Figure 6 also shows the typical far-field directivity pattern of aircraft high lift system noise. The broad directivity is typically observed for airframe noise[2,6,18,19] and is very representative of all of our data. The maximum radiation occurs in the fly-over direction right below the aircraft, but the falloff away from this direction is very gradual. As is shown in Fig. 6, even at positions 60 deg away from the maximum radiation direction, the noise levels are still less than 5 dB lower than the maximum. This broad directivity is again a result of the multiple sources associated with the high lift systems. As analyzed in Refs. 9 and 15, individual sources related to slats and flaps also have broad directivity but have maximum radiation in different directions. For slat sources the maximum radiation is in the aft quadrant, whereas for the flap sources radiation peaks in the forward quadrant. The aggregated effects of all of these sources then lead to the broad directivity.

IV. Effects of High Lift System Configurations

As can be expected intuitively, the noise levels also depend on the high lift system configurations, namely, the slats and flaps. In general, our data show that the deployment of any components of the high lift system increases the noise level and the larger the deployment angle, the higher the noise levels. This is clearly shown in Figs. 7 and 8; Fig. 7 shows the effects of flap angles, whereas Fig. 8 illustrates the dependence of the noise levels on the slat deployment. The cases shown in these figures all have mean flow Mach number $M = 0.275$ and all with landing gears retracted. The far-field microphone is right below the wing at 84 deg from the upstream direction. Figure 7 plots far-field noise spectra at different flap angles; the upper diagram is for the case with slats retracted, and the lower diagram for the case with slats deployed at 20 deg. For Fig. 8, the top, middle, and bottom plots are, respectively, for flap angles of 25, 35, and 50 deg. In all three plots the upper curves (with squares) are for the cases of slats deployed at 20 deg, whereas the lower curves (with circles) are for the cases of slats retracted.

Both Figs. 7 and 8 show that the increase in noise levels caused by the slat/flap deployment is frequency dependent. The upper plot in Fig. 7 shows the effects of flap angles without any other significant sources (slats retracted). In this case the increase in the flap

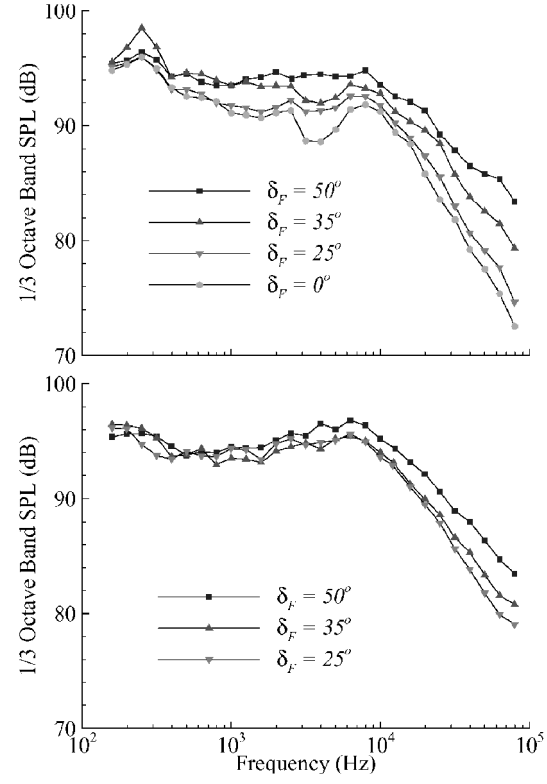

Fig. 7 Dependence of far-field noise spectra on flap angles for microphone location right below the wing (84 deg from upstream direction). All results are for Mach number $M = 0.275$ and landing gears retracted. The upper diagram is for slats retracted and the lower for slats at 20 deg.

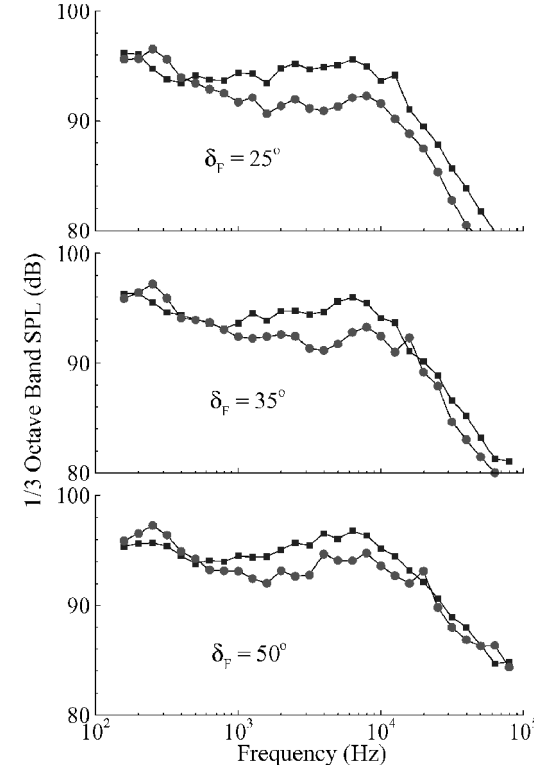

Fig. 8 Slat-angle dependence of far-field noise spectra below the wing (84 deg from upstream direction). All results are for Mach number $M = 0.275$ and landing gears retracted. The top, middle, and bottom diagram are, respectively, for flap angles of 25, 35, and 50 deg. The curves with squares are for slats at 20 deg, and those with circles are for slats retracted.

deployment angle causes the noise to increase in almost the entire frequency range, from about a few hundred hertz to 100 kHz. The higher the frequency is, then the higher the increase in noise levels. The increase can be as high as 10 dB in the frequency range shown, as the flap angle increases from 0 to 50 deg. When the slats are deployed at 20 deg, however, the effects of changing the flap angles are quite different, as shown in the lower plot in Fig. 7. In this case the increase in noise levels caused by the flap angles is mainly confined to the high frequencies above about 10 kHz. Below that, no significant increase in noise levels is seen. This is because the noise in the low- and midfrequency domain in this case is dominantly radiated by sources associated with the slats. These sources depend mainly on conditions of the slats and are not sensitive to changes of the flaps. The high-frequency components are still generated by the flaps so that the noise levels in this frequency domain still change significantly with the flap angle.

This effect of the slats can also be seen in Fig. 8; the bottom plot shows a noticeable increase in noise level in the midfrequency domain when the slat angle changes from 0 to 20 deg. The high-frequency components are not affected by the slat angles because these components are dominantly generated by sources related to the flaps, which are deployed at 50 deg for this plot. The slat effects in the midfrequency domain are seen for all flap settings in the three plots in Fig. 8, with slightly more increase in noise levels at small flap angles. The most significant effects of the slats at high frequencies come from the case of low flap settings, for example, the top plot in Fig. 8. In this case the sources caused by the flaps are relatively weak so that the slat sources also contribute significantly to the high-frequency noise, which is why the deployment of the slats can significantly increase the high-frequency noise as shown in this plot. This is particularly of interest to modern airplanes, which usually have simple flap systems and small flap settings. For airplanes of this kind, our data indicate that slat noise might be the most important component for high lift system noise.

V. Source Identification Map by Phased Microphone Array

Whereas the technique of phased microphone arrays has seen many applications in aircraft noise research, it is by no means a mature measurement method in that the interpretation of its results still requires considerable understanding and calibration. Because of this, it is appropriate to point out that our objective of analyzing the phased microphone array data is not to derive any quantitative results. Instead, our focus is on the identification of major source locations in the aircraft high lift systems and the analysis of the source variations with high lift system configurations and flow conditions. Furthermore, our results are calibrated with those from other measurement techniques, such as free field microphones and unsteady surface pressure sensors. As will be seen in this and the next section, the results on source variations reveal trends quite consistent with the analysis of far field microphone data, given in earlier sections. The identification of source locations is also consistent with the far-field/near-field correlation analysis.[5]

The phased microphone array data are originally processed so that source strengths can be mapped at any frequency below 20 kHz because of limitations in our data acquisition system.[20,21] The narrowband data, however, show quite significant fluctuations from frequency to frequency, making the interpretation of the results very difficult. To smooth out the fluctuations, and to be consistent with common practice in airframe noise studies, the source strength maps are converted to $\frac{1}{3}$-octave band source spectra. A representative example of the source strength maps derived from the array data is shown in Fig. 9. This is for the case of flow Mach number $M = 0.275$, flaps and slats, respectively, deployed at 50 and 20 deg, and landing gears retracted. Each plot gives the source strengths for one $\frac{1}{3}$-octave band with its center frequency indicated on the plot. To show the locations of the major sources for each frequency band most clearly, the source levels are different for each plot, but all plots have the same dynamic range of 10 dB. This is done because maximum source levels at different frequencies differ quite significantly; if the same levels were used for all plots, the sources at some

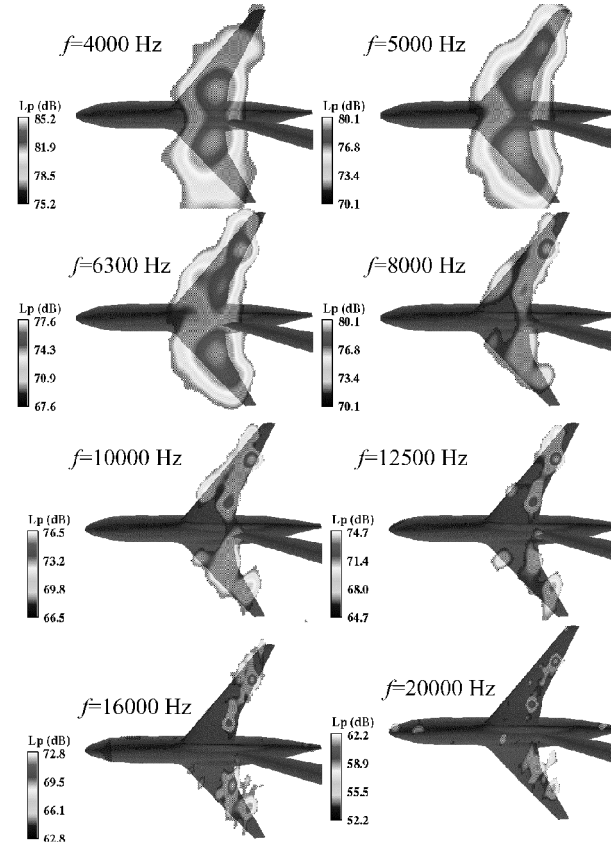

Fig. 9 One-third octave band noise source strengths for the case of Mach number $M = 0.275$, flaps and slats deployed, respectively, at 50 and 20 deg, and landing gears retracted.

frequencies would be extremely difficult to show up because of their low levels compared with those at other frequencies.

It can be noticed that the source strength maps are not symmetrical with respect to the fuselage centerline. This is probably because of one or both of the following two reasons: The first is simply the fact that the array location in the test setup is not right below the aircraft model and the distances from the array to any two corresponding points on the two wings are different. This difference is not corrected in the array data processing so that even two identical sources at two corresponding points on the wings would appear to be different. However, because our objective here is to identify major source locations and to show relative variations in source strength for different aircraft configurations and flow conditions this artifact from array data processing is not a real concern. The second possible reason for the nonsymmetrical source strength maps might be the directivity of the flap edge sources. As shown in the color maps, the port wing usually shows a higher source level at the outboard edges of the flaps than the starboard wing. This might be caused by strong directivity effects of these sources. A semibaffled dipole model that is oriented at the flap edge (perpendicular to the flight direction) would result in strong radiation in the direction of the microphone array from the port wing and relatively weak radiation from the starboard wing, causing the nonsymmetrical array maps. Because all of the beam-forming data processing assumes monopole radiators, this source directivity issue cannot be resolved if it turns out be the true reason for the nonsymmetry.

Starting from top left plot in Fig. 9, it can be seen that at low frequencies, for example, 4 kHz, the major sources are located in the region close to the hubs of the wings, which includes the thrust gate with two flap side edges. The source maps show that the sources are distributed quite extensively, covering the entire chord length of the wing. Clearly, this makes it difficult to interpret the source. Furthermore, the extensive source region might also be caused by the limited array resolution at these low frequencies. For frequencies above 5 kHz, the source maps very clearly show the importance of

the flap side edges as major source regions; high source levels show up in these regions for all frequencies all way up to 20 kHz. In the midfrequency domain between 5 and 12.5 kHz, high source levels are also seen in the region near the leading edge of the wing, resulting from sources related to the slat flow. All of these are quite consistent with the results derived from the analysis of free microphone data; flap-related noise is seen there to cover the entire mid- and high-frequency domain, whereas slat noise mainly manifests itself in the midfrequency region. In the mid- and high-frequency domain it is also clear that the outboard edge of the outboard flap is a strong source. This has also been confirmed by correlation analysis between far-field noise and pressure fluctuations on the flap surface.[5] It can be seen, for example, from the plot for 10 kHz, that the slat sources have lower amplitudes than those related to the flaps but are quite extensively distributed in space. In the plot for 10 kHz, the leading-edge slat sources cover almost the entire slat region, in contrast to the flap sources, which are highly concentrated. The individual source amplitude for the slat sources is about 5 dB lower than the maximum amplitude of the flap sources.

VI. Component Analysis

The source strength plots in Fig. 9 reveal four subregions on the wing that are of particular interest, namely, the inboard flap close to the fuselage, two side edges of the outboard flap, and the slat region. To reveal the variations of the sources with changes in high lift system configurations and flow conditions, the source strengths such as those shown in Fig. 9 are integrated over these four respective subregions. The integration subregions are illustrated in Fig. 10. The integration is done by simply adding the sources in the subregions incoherently, namely, the source strengths are integrated on the energy base (pressure squared). This is a reasonable assumption for airframe noise whose sources are mostly incoherent and broadband in nature. For the case shown in the Fig. 9, namely, for $M = 0.275$, flaps and slats, respectively, deployed at 50 and 20 deg and landing gears retracted, the integrated source spectra are plotted in Fig. 11, respectively, for the four subregions as a function of frequency. We choose to work with integrated source spectra, instead of individual source amplitude, because the integrated strength is a more accurate measure of the effects on the far-field noise; the noise is the sum of the radiation from all of the sources.

When the source strengths are integrated, the relative importance of different components can be quite different from that derived from the amplitudes at individual points such as those shown in Fig. 9. In these figures the maximum source strengths, namely, the maximum contour level, are mostly identified to be at the outboard edge of the outboard flap. The integrated results in Fig. 11, however, show that the slat subregion is consistently comparable to or stronger than those related to the flaps in all frequency bands. This can be easily explained by the fact that sources associated with slats have a very extensive spatial distribution, whereas those related flaps are quite

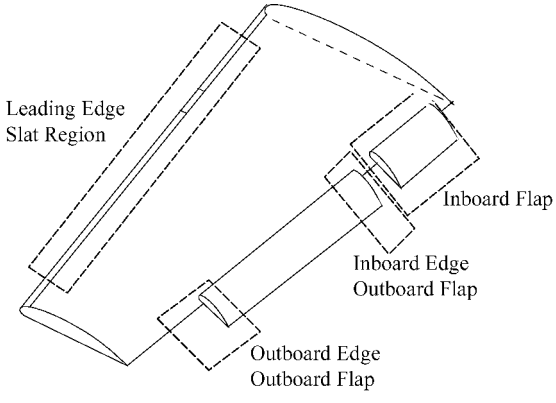

Fig. 10 Illustration of the subregions for source strength integration. The wing is divided into four subregions: the outboard edge of the outboard flap, the inboard edge of the outboard flap, the inboard flap, and the slat.

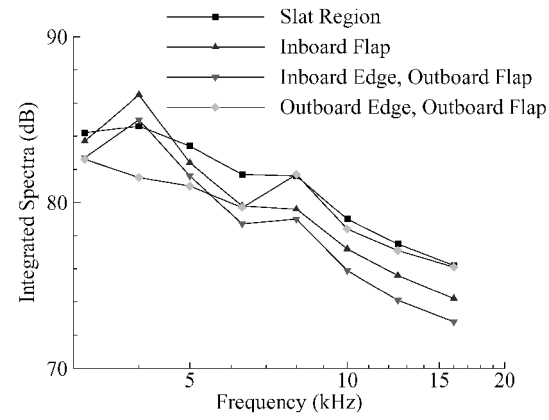

Fig. 11 Source spectra integrated from phased microphone array data for the four subregions shown in Fig. 10 for the case of Mach number $M = 0.275$, flaps and slats deployed, respectively, at 50 and 20 deg, and landing gears retracted.

concentrated in space; the integrated effects can then be quite different from the comparison between single points in the respective source regions. This also demonstrates the need for caution when interpreting results from phased microphone array measurements. It is sometimes misleading to regard the most intense source identified by the phased microphone array as the most significant contributor to the far-field noise. This is because, in the presence of distributed sources, most or a large part of the noise can come from the integration of the source distributions, even though their source density (source strength per unit volume) might not be the highest.

The integrated source strengths can also be utilized to study the dependence of the sources on high lift system configurations. In general, the variations in noise source strengths caused by changes in slats and flaps are consistent with the trends revealed in the far-field spectra, as discussed in preceding sections. The integrated array results can add more insight to those far-field trends because the sources in the subregions can be separated. An example is given in Fig. 12 to show the effects of flap angles on the strengths of the four source regions. For the three subregions on the flaps, the source levels are evidently affected by the flap angles; the higher the flap angle is, the higher the source levels, consistent with the far-field trends analyzed in the preceding sections. The sources in the slat region, however, do not seem to be affected by the flap angle changes, as clearly demonstrated in the top diagram of Fig. 12. By comparing the levels of the curves for the lowest flap setting ($\delta_F = 25$ deg, indicated by diamonds) in all four of the plots in Fig. 12, it is clear that the slat sources are the most important. This is again consistent with our far-field analysis; as the flap-related sources become less strong at low flap settings, the slats take over the leading role in generating high lift system noise. This can be of importance for more recent aircraft types that typically use much smaller flap defection angles than the DC-10 model.

The effects of the slat deployment on the noise source levels are shown in a similar way in Fig. 13. The comparison here is between the case with slats retracted and that with slats deployed at 20 deg. Other conditions for the two cases are exactly the same, namely, $M = 0.275$, flaps deployed at 50 deg, and landing gears retracted. Apparently, the comparison immediately reveals that the levels of noise sources in the slat region are significantly reduced when the slats are retracted, up to 6 dB. However, the sources associated with the flaps are much less affected by the slat angles, as can be expected. For instance, the inboard flap region actually has an increase in the levels of noise sources at higher frequencies, and the sources at the outboard edge of the outboard flap only have a small reduction in level above 8 kHz. It can be seen from Fig. 12 that the effects of flap angles on slat sources are basically negligible, but Fig. 13 shows that the slat angles have some effects on the flap sources. This is probably because the slats are located upstream of the flaps so that the aerodynamic coupling, which affects the source strength, is stronger from slats to flaps than the other way around.

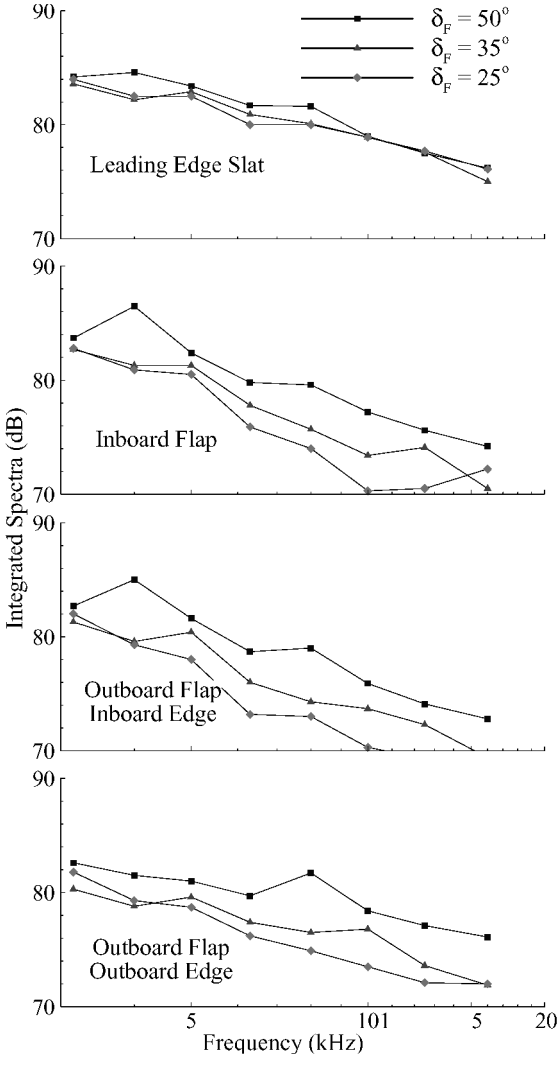

Fig. 12 Effects of flap angles on the source spectra integrated from phased microphone array data in different subregions, for the case of Mach number $M = 0.275$, slats deployed at 20 deg, and landing gears retracted.

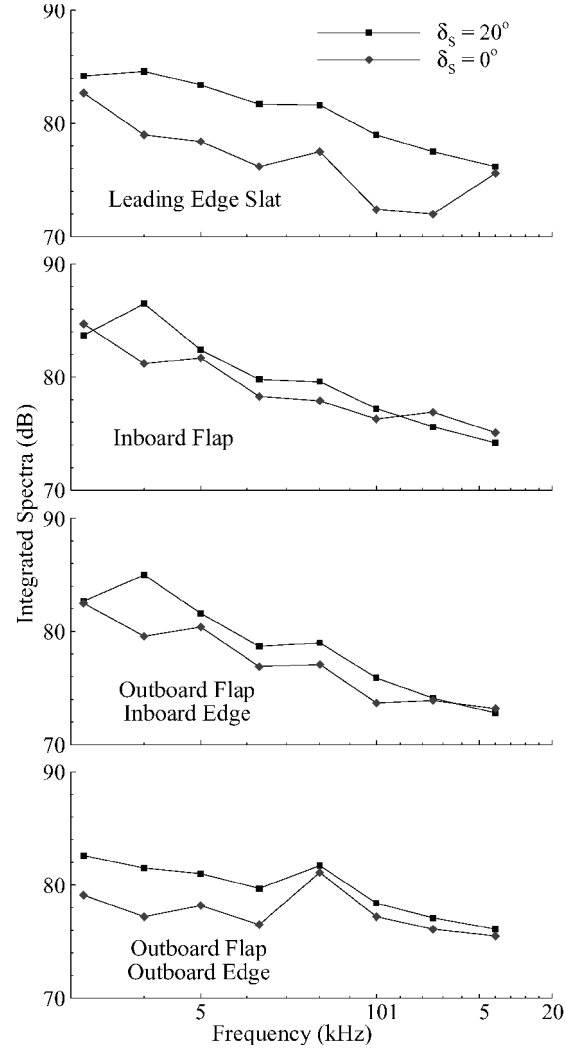

Fig. 13 Effects of slat angles on source spectra integrated from phased microphone array data in different subregions, for the case of Mach number $M = 0.275$, flaps deployed at 50 deg, and landing gears retracted.

VII. Effects of Flap Side Edge Fences

In recent years flap side edge fences have been studied as a noise-reduction device, both on simple flap models[22] and in fly-over test of real airplanes.[21] Though the exact mechanisms by which noise is reduced are not fully understood, it is commonly accepted that fences can reduce flap-related noise by a noticeable amount. This is confirmed in our test. Some results are shown in Fig. 14 for the cases of flow Mach number $M = 0.275$, flaps at 50 deg, and both with (lower plot) and without (upper plot) slats deployed. The fences are shown here to be most efficient for high frequencies, both with and without slats. This is because the noise of the DC-10 aircraft model is dominated by flap-related sources, which is mainly in the high-frequency domain. Also note that the reduction when the slats are retracted is slightly higher (about 1 dB) than that when the slats are deployed, apparently because the fences only affect the noise components from the flaps. The effects of different fence heights are also shown in this figure. For the three fences tested, it seems that large fences have the most noise reduction. However, the amount of noise reduction does not increase linearly with the fence height. From the case without fence to that with the $\frac{1}{2}$-thickness fence, a significant reduction is achieved. As the fence height increases, the increase in noise reduction becomes very gradual. This is especially clear in the lower plot of Fig. 14; doubling the fence height from one to two flap-thickness does not seem to yield any benefit.

From the noise spectra at all far-field angles, the radiated noise can be calculated in terms of EPNL, which is an important metric in aircraft noise certification. For the cases shown in the top plot of Fig. 14, the reduction in EPNL is about 4 dB. This is clearly quite significant. It is, however, appropriate to point out that the reduction is for flap-related noise only with both the slats and the landing gears retracted, both being known to be also important airframe noise sources. In practical application of total aircraft noise consisting of many other components, the reduction in EPNL decibels can be expected to be much less. This is especially true for cases where the flaps are not the dominant sources. Examples are new commercial airplanes developed in recent years, such as the Boeing 777, which have relatively low flap settings. In this case the total airframe noise would not be very sensitive to flap side edge treatment such as the fences.

One can see from Fig. 14 that although the fences are effective in reducing high-frequency noise they actually increase the noise level at low frequencies. For example, the case with the two-thickness fence (the curve with diamonds in the top plot of Fig. 14) has higher noise levels at low frequencies than all other cases, including that without fence. From our unsteady surface pressure data[5] we find that the maximum levels in the surface-pressure spectra are also shifted downward in frequency when the fences are applied. This can provide a possible explanation for the role of the flap side edge fences. The downward shift of dominant frequency might be caused by the effective increase of the flap thickness by the fences. The features of sources are essentially determined by the characteristic time of

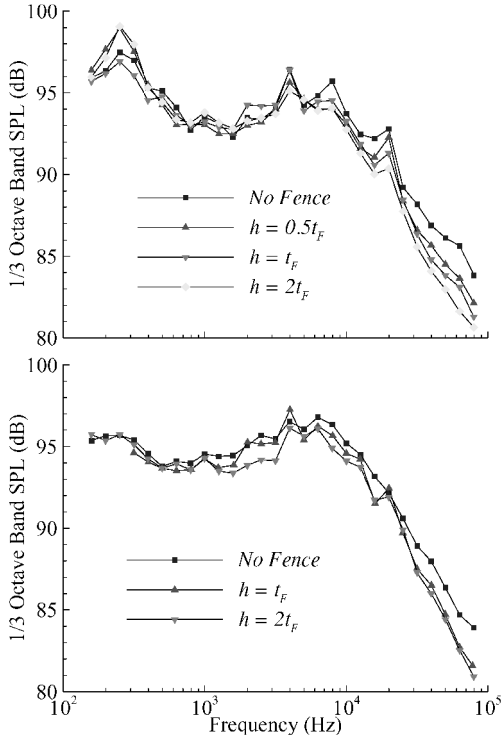

Fig. 14 Effects of flap side edge fences on far-field noise spectra below the wing (84 deg from upstream direction). All results are for Mach number $M = 0.275$ and landing gears retracted. The upper diagram is for slats retracted, and the lower for slats at 20 deg.

the fluctuations in the flap side edge flow. With increased dimension in the thickness direction caused by the attachment of the fences, the flow has more time to evolve before it has to interact with the sharp corners. Correspondingly, the flow has lower characteristic frequencies. This leads to a downward shift of the spectra of both near-field pressure and far-field noise from the case without fences. Even without any reduction in source strengths, this downward shift in frequency can appear as a noise reduction. This is because airframe noise typically has a spectrum with a negative slope in almost the entire mid- to high-frequency domain, which is also the most sensitive domain for aircraft noise certification. Thus, for any fixed frequency bands a downward shift of the spectrum replaces the noise levels in these bands with the lower levels at higher frequencies. In this way a reduction in noise level is achieved for fixed-frequency bands even if the total radiated acoustic energy remains unchanged. It is appropriate to point out that our limited database does not enable us conclusively to show whether there is a weakening in source strength as a result of the fences, which might also contribute to the observed reduction in far-field noise. Our data, however, do reveal the downward shift in characteristic frequencies of the flow features. This indicates that at least some part of the noise reduction caused by flap side edge fences comes from the shift of the acoustic energy out of the frequency bands that are important to aircraft noise certification.

VIII. Conclusions

In this paper some major trends in the far-field noise of aircraft high lift systems have been analyzed by making use of both far-field free microphone data and measurements from a phased microphone array. Some of these trends might be specific to the DC-10 aircraft model, whereas others are quite general with applications to other types of aircraft. It has been shown that the noise scales on the flow Mach number according to the fifth and sixth power law, respectively, in the low-to-mid- and high-frequency domains. This is because the slats and flaps are dominant noise sources in these two respective frequency domains. For slat noise the approximately two-dimensional geometry can introduce two-dimensional sources, yielding the fifth power scaling law, and for flap noise the radiation is typically that of the dipole type caused by unsteady pressure fluctuations on the flaps, which leads to the sixth power law. Although the main wings might be the main noise sources for clean configurations with all high lift devices retracted, it has been shown that for the more practical cases with flaps and/or slats deployed the flaps and/or slats dominate the far-field radiation. Concentrated high-frequency noise sources have been identified in the flap side edge regions, and the slats have been shown to be responsible for distributed noise sources of low- to midfrequencies. The far-field noise has been shown to have a strong dependence on the high lift system configurations. In general, the higher the deployment angle of any of the components in the high lift systems is, the higher the noise levels. In terms of the total noise, for example, the effective perceived noise level, the flaps are most important at high flap deflection angles. The leading role in generating noise, however, is largely taken over by sources associated with the slats at moderate and low flap deflection angles, a trend confirmed not only by far-field data but also by phased microphone array measurements. This is probably a feature of interest to aircraft types developed in recent years, whose flap settings are usually lower than that of the DC-10 model.

It has been demonstrated that flap side edge fences are effective at reducing noise related to flap side edges for the DC-10 aircraft model. The reduction can be as high as 4 dB at some frequencies. Our data have shown some evidence that this reduction can come from a downward shift of the noise spectra, which itself can be caused by a similar shift in the source spectra, resulting from the increased characteristic length scale of the flow causede by the fences. The fences are less effective in reducing the total airframe noise because they have negligible effects on the slat sources that might be the dominant or a major contributor to the total airframe noise.

Acknowledgments

The work presented in this paper is sponsored by the NASA Advanced Subsonic Technology Program (under the Noise Reduction Element). The authors thank the Task Monitor, W. C. Horne of NASA Ames Research Center, Moffett Field, California, for his support and encouragement. The authors also thank the group of people at NASA Ames Research Center who made the test a success: C. J. Ross, P. T. Soderman, D. Ashby, B. L. Storms, J. A. Hayes, M. Watts, and M. Mosher, to name just a few. Paul Bent was the test engineer from Boeing, whose contributions are gratefully acknowledged.

References

[1]Hardin, J. C., "Airframe Self-Noise-Four Years of Research," AGARD Lecture Series No. 80 on Aerodynamic Noise, Dec. 1976.

[2]Fink, M. R., "Noise Component Method for Airframe Noise," *Journal of Aircraft*, Vol. 16, No. 10, 1979, pp. 659–665.

[3]Kendall, J. M., and Ahtye, W. F., "Noise Generation by a Lift Wing/Flap Combination at Reynolds Numbers to 2.8 Million," AIAA Paper 80-0035, Jan. 1980.

[4]Crighton, D. G., "Airframe Noise," *Aeroacoustics of Flight Vehicles: Theory and Practice*, NASA RP-1258, Vol. 1, edited by H. H. Hubbard, 1991, pp. 391–447.

[5]Guo, Y. P., Joshi, M. C., Bent, P. H., and Yamamoto, K. J., "Surface Pressure Fluctuations on Aircraft Flaps and Their Correlation with Far Field Noise," *Journal of Fluid Mechanics*, Vol. 415, 1999, pp. 175–202.

[6]Bauer, A. B., and Munson, A. G., "Airframe Noise of the DC-9-31," NASA CR 3027, Dec. 1978.

[7]Ffowcs, Williams, J. E., and Hall, L. H., "Aerodynamic Sound Generation by Turbulent Flow in the Vicinity of a Scattering Half-Plane," *Journal of Fluid Mechanics*, Vol. 40, 1970, pp. 657–670.

[8]Howe, M. S., "A Review of the Theory of Trailing Edge Noise," *Journal of Sound and Vibration*, Vol. 61, No. 3, 1978, pp. 437–465.

[9]Guo, Y. P., "A Model for Slat Noise Generation," AIAA Paper 97-1647, May 1997.

[10]Ffowcs, Williams, J. E., "Hydrodynamic Noise," *Annual Review of Fluid Mechanics*, Vol. 1, 1969, pp. 197–222.

[11]Crighton, D. G., "Basic Principles of Aerodynamic Noise Generation," *Progress in Aerospace Sciences*, Vol. 16, No. 1, 1975, pp. 31–96.

[12]Guo, Y. P., "Application of Ffowcs Williams/Hawkings Equation to Two-Dimensional Problems," *Journal of Fluid Mechanics*, Vol. 403, 2000, pp. 201–221.

[13]Hardin, J. C., "Noise Radiation from the Side Edges of Flaps," *AIAA Journal*, Vol. 18, No. 5, 1980, pp. 549–552.

[14]Sen, R., "Local Dynamics and Acoustics in a Simple 2D Model of Airfoil Lateral-Edge Noise," AIAA Paper 96-1673, May 1996.

[15]Guo, Y. P., "Prediction of Flap Edge Noise," AIAA Paper 99-1804, June 1999.

[16]Curle, N., "The Influence of Solid Boundaries upon Aerodynamic Sound," *Proceedings of the Royal Society of London*, Vol. A231, 1955, pp. 505–514.

[17]Ffowcs Williams, J. E., and Hawkings, D. L., "Sound Generation by Turbulence and Surfaces in Arbitrary Motion," *Philosophical Transactions of the Royal Society of London*, Vol. A264, 1969, p. 321.

[18]Sen, R., Blackner, A. M., Yee, P., and Stocker, R., "Airframe Noise Generation and Radiation," NASA CR NAS1-20090, Oct. 1996.

[19]Yamamoto, K. J., Donelson, M. J., Huang, S. C., and Joshi, M. C., "Airframe Noise Prediction Evaluation," NASA CR 4695, Oct. 1995.

[20]Mosher, M., "Phased Arrays for Aeroacoustic Testing: Theoretical Development," AIAA Paper 96-1713, May 1996.

[21]Ross, J. C., Storms, B. L., and Kumagai, H., "Aircraft Flyover Noise Reduction Using Lower-Surface Flap-Tip Fences," NASA CDTM-21006, Oct. 1995.

[22]Storms, B. L., Takahashi, T. T., Horne, W. C., Ross, J. C., Dougherty, R. P., and Underbrink, J. R., "Flap-Tip Treatments for the Reduction of Lift-Generated Noise," NASA CDTM-21006, Oct. 1996.

[23]Hayes, J. A., Horne, W. C., Soderman, P. T., and Bent, P. H., "Airframe Characteristics of a 4.7% Scale DC-10 Model," AIAA Paper 97-1594, June 1997.

[24]Hayes, J. A., Horne, W. C., Jaeger, S. M., and Soderman, P. T., "Measurement of Reynolds Number Effect on Airframe Noise in the 12-Foot Pressure Wind Tunnel," AIAA Paper 99-1959, June 1999.

[25]Allen, C. S., and Soderman, P. T., "Scaling and Extrapolating Small-Scale In-Flow Wind Tunnel Jet Noise to Full Scale Fly-Over Jet Noise," AIAA Paper 97-1602, May 1997.

A. Plotkin
Associate Editor